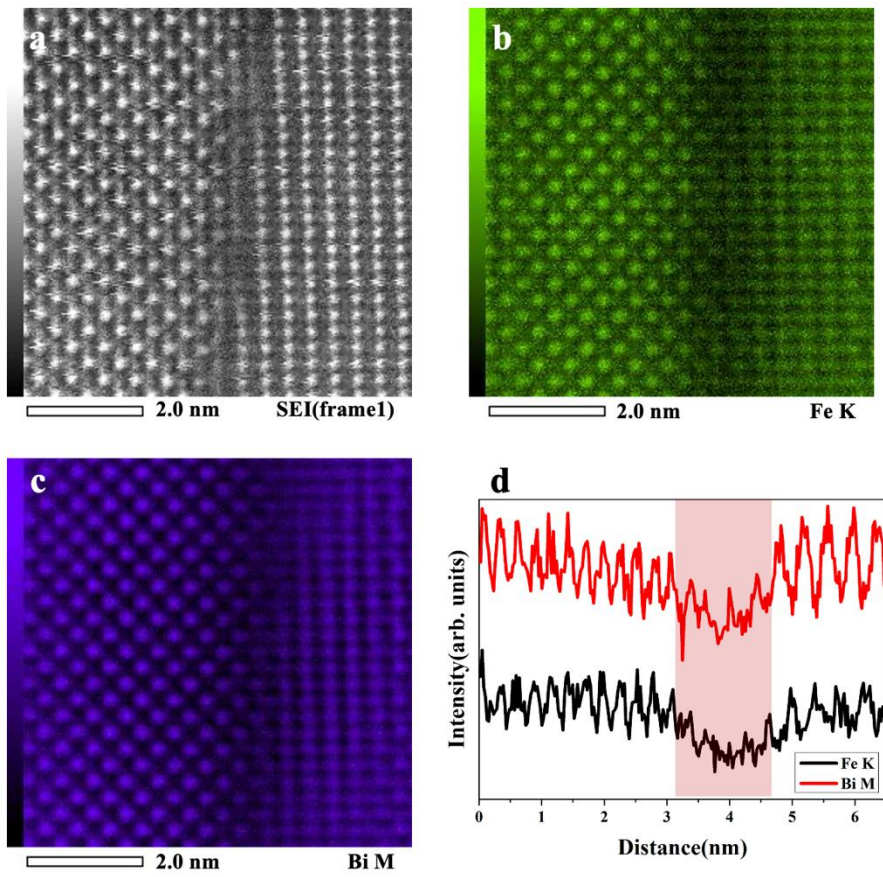
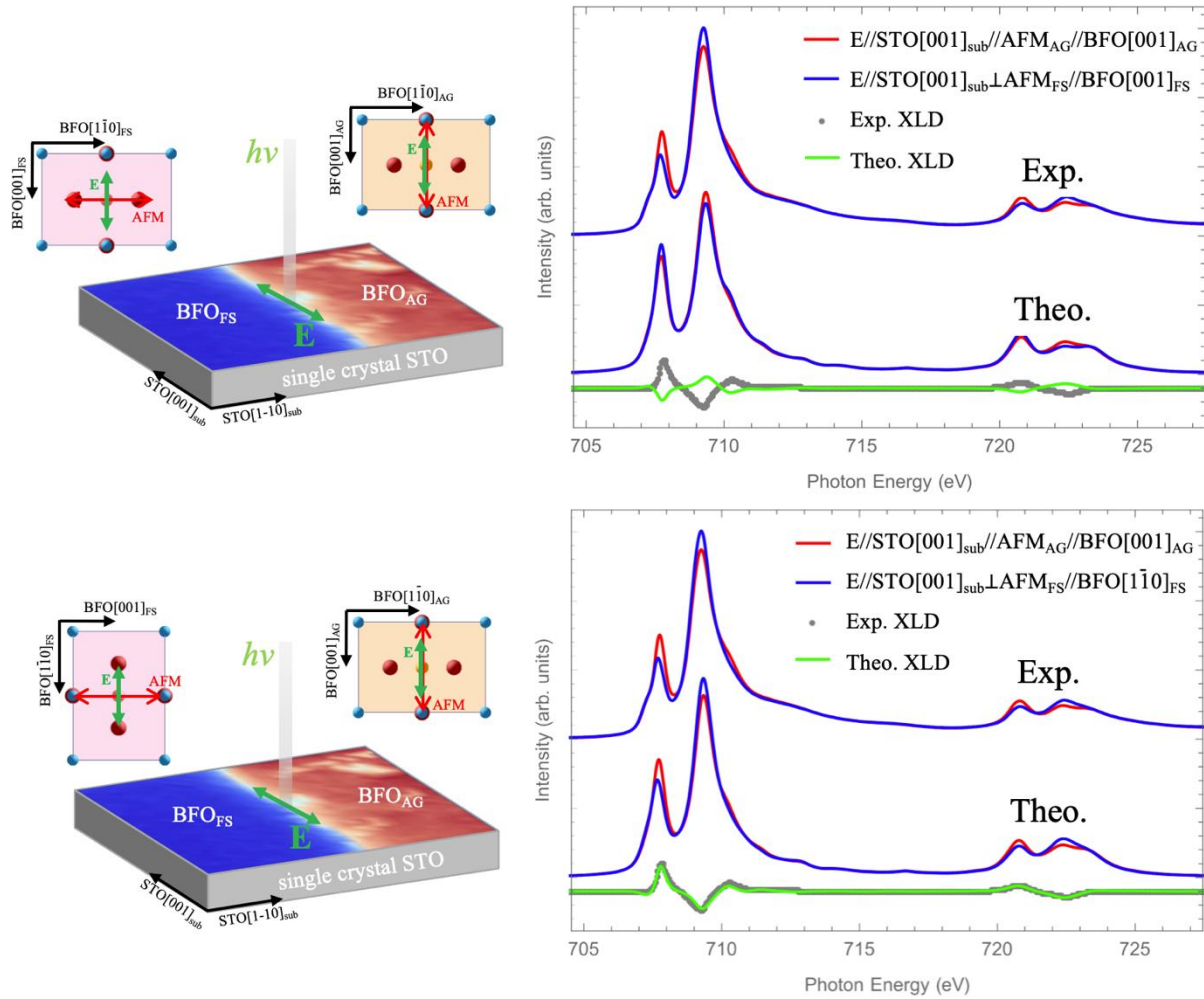


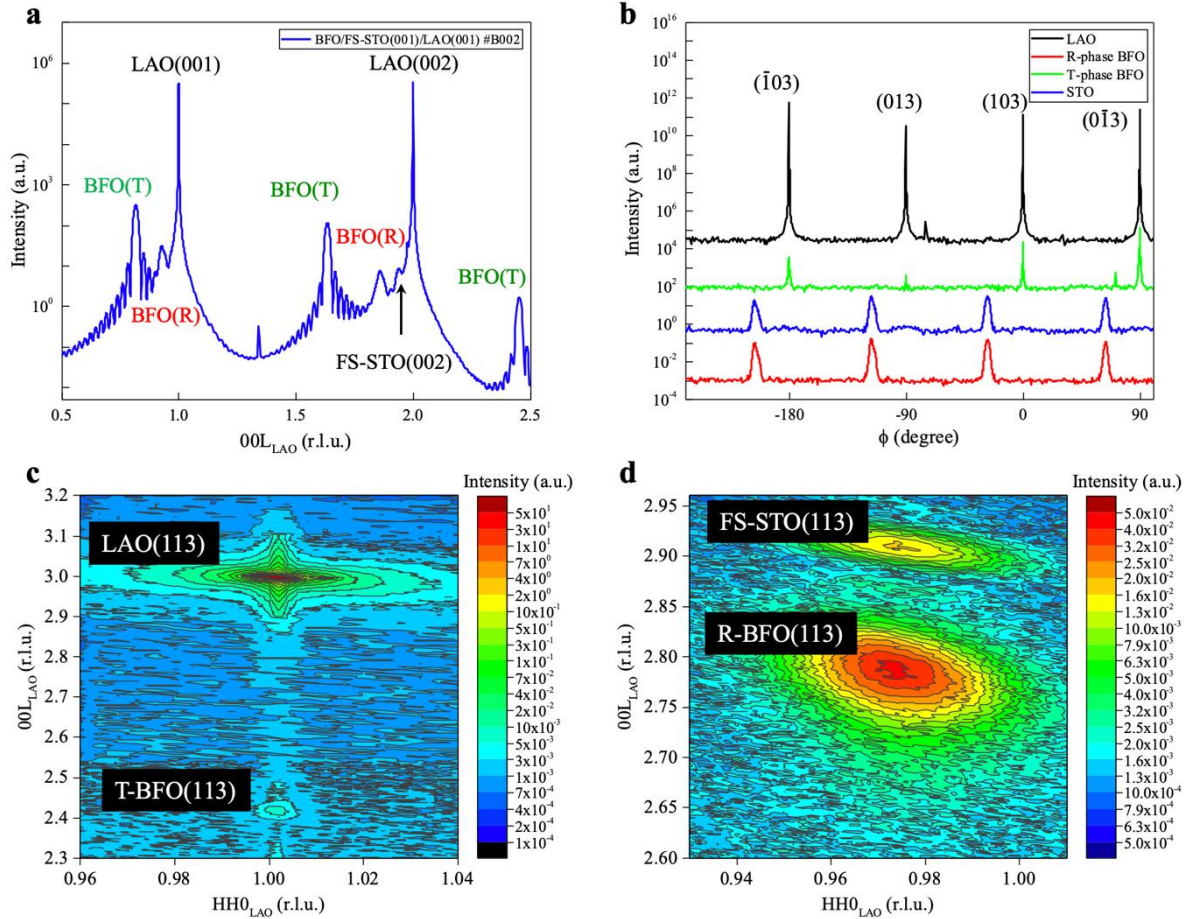
**Extended Data Fig. 1 | X-ray Diffraction (XRD) of the Heteroepitaxy.** **a** XRD normal scan of twist BFO homostructure on (110)-oriented STO substrate indicates pure (110)-oriented BFO peaks without any secondary phase. **b** XRD in-plane  $\phi$ -scan of STO {221} and BFO {221}. The detection of 4 peaks in STO {221} planes indicates the contributions from both freestanding and single crystal STO substrate areas. In the present sample, the twist angle between single crystal STO substrate and freestanding STO is  $\sim 85^\circ$ .



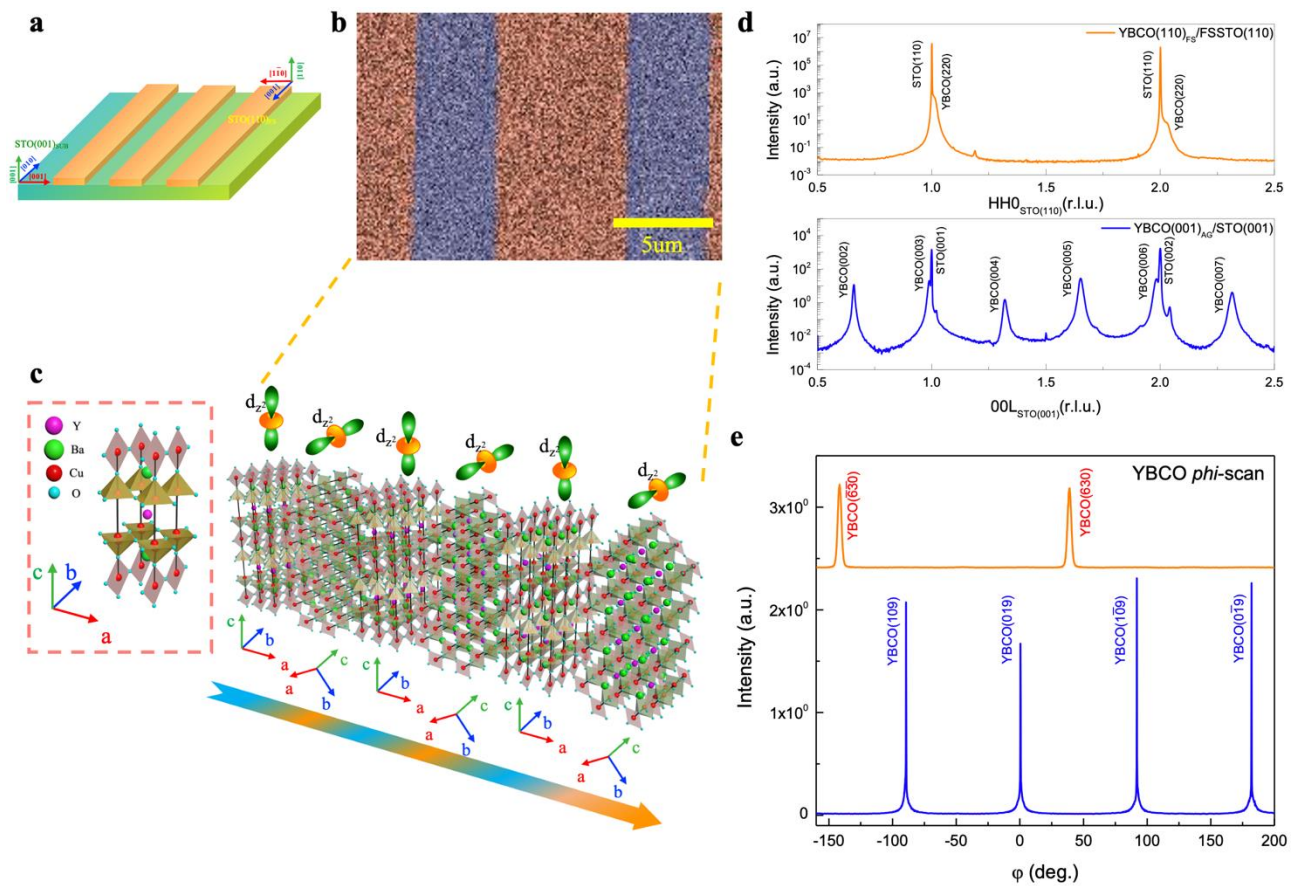
**Extended Data Fig. 2 | Atomic resolved EDS map.** **a** HAADF-STEM image of the interface region in the BFO<sub>AG</sub>/BFO<sub>FS</sub>. **b** and **c** Atomic resolved Fe and Bi EDS map. **d** Line profiles of Fe and Bi extracted from the mapping.



**Extended Data Fig. 3 | Fe  $L_{2,3}$ -edge X-ray absorption and linear dichroism spectra of  $\text{BFO}_{\text{AG}}$  and  $\text{BFO}_{\text{FS}}$  with  $E//\text{STO}[001]_{\text{SUB}}$ .** The red and blue lines in the upper right and lower right panels represent the absorption spectra of  $\text{BFO}_{\text{AG}}$  and  $\text{BFO}_{\text{FS}}$ , respectively; while the green lines and gray dots show the experimental and simulated dichroism spectra, respectively. For the calculated spectra in the upper panel, only the  $90^\circ$  rotation of antiferromagnetic axis from  $\text{BFO}_{\text{AG}}$  to  $\text{BFO}_{\text{FS}}$  was considered, as illustrated in the left schematic. On the contrary, for the calculated spectra in the lower panel, both the  $90^\circ$  rotation of antiferromagnetic axis and the rotation of  $[1\bar{1}0]$  crystallography-axis from  $\text{BFO}_{\text{AG}}$  to  $\text{BFO}_{\text{FS}}$  were considered, as illustrated in the left schematic.



**Extended Data Fig. 4 | X-ray diffraction of BFO grown on STO/LAO twist template.** **a** XRD normal scan along LAO (001). The characteristic peaks of R-BFO, T-BFO, FS-STO, LAO are labeled accordingly in the figure. **b** The XRD in-plane  $\phi$ -scans along  $\{103\}$  planes of R-BFO, T-BFO, STO, and LAO indicate the well-aligned epitaxial relationship of R-BFO/FS-STO and T-BFO/LAO, respectively. **c** The RSM around  $\{113\}$  plane of LAO revealed the single domain feature of T-BFO and the T-BFO is fully strained by LAO substrate **d** The RSM around  $\{113\}$  plane of STO also indicates a strained R-BFO phase on FS-STO.



**Extended Data Fig. 5 | Patterned twisted YBCO lateral homostructures.** **a** The designer periodic arrays of twisted template composed by (110)<sub>FS</sub>- (001)<sub>SUB</sub>- oriented STO. Firstly, a STO twisted template was prepared with (001)-oriented STO substrate overcovered by freestanding (110)-oriented STO layer. The stripe patterns with periodic arrays were then manufactured through the combination of etching and photolithography. **b** Scanning electron microscopy image of patterned YBCO homostructure grown on the designer twisted STO template. **c** Schematic illustration of the crystal arrangement and representative  $d_{z^2}$  orbital configuration of the twisted YBCO lateral homostructures. **d** XRD normal scans of YBCO films grown on (110) FSSTO (orange line) and on (001) STO substrate (blue line) area. The homostructure exhibits crystal structure of (001)- and (110)-oriented YBCO on (001)<sub>SUB</sub>- and (110)<sub>FS</sub>-oriented STO, respectively, which is nicely consistent with the designed crystal geometry. **e** XRD in-plane phi-scan of {630} plane of (110)-oriented YBCO and {109} plane of (001)-oriented YBCO, revealing the corresponding two-fold and four-fold symmetry of YBCO grown on the designer twisted STO template.